


## Article

# Spatiotemporal Evolution Characteristics of Urbanization in the Xiamen Special Economic Zone Based on Nighttime-Light Data from 1992 to 2020

Chunfang Chai <sup>1,2</sup>, Yuanrong He <sup>1,3,\*</sup>, Peng Yu <sup>1,3</sup> , Yuanmao Zheng <sup>1,2</sup>, Zhicheng Chen <sup>4</sup>, Menglin Fan <sup>1,2</sup> and Yongpeng Lin <sup>1,3</sup>

<sup>1</sup> Big Data Institute of Digital Natural Disaster Monitoring in Fujian, Xiamen University of Technology, Xiamen 361024, China

<sup>2</sup> School of Environmental Science and Engineering, Xiamen University of Technology, Xiamen 361024, China

<sup>3</sup> College of Computer and Information Engineering, Xiamen University of Technology, Xiamen 361024, China

<sup>4</sup> Xiamen Urban Planning and Design Institute Co., Xiamen 361012, China

\* Correspondence: 2012112001@xmut.edu.cn

**Abstract:** In China and elsewhere, urban expansion is directly related to the important issues of social development, economic development, and the sustainable development of the ecological environment. Traditional statistical methods based on administrative regions lack geospatial information, which makes it difficult to analyze and explore in detail the development status and spatial differences of cities. In real time, nighttime light (NTL) remote sensing can reveal the spatial expansion change information of urban built-up areas (UB) on different scales, thus allowing for the analysis of urban spatial patterns and variations in urban development. Based on the long-time sequence NTL data from 1992 to 2020, this work studies the Xiamen Special Economic Zone by using the vegetation-water-adjusted NTL urban index (VWANUI) to extract the urban built-up areas and study the UB expansion patterns, the migration of the urban center of gravity, and intra-city differences. The result is a qualitative and quantitative temporal and spatial evaluation of Xiamen's economic development characteristics. The results show that the UB of Xiamen expanded 349.219 km<sup>2</sup> from 1995 to 2020, mainly concentrated in the period 2005–2020, during which time 79.44% of the expansion of the whole study period occurred. Throughout the study period, the urban center of gravity of Xiamen city shifts 8757.15 m to the northeast at the rate of 350.29 m/year in the direction of 74.88° (the urban center of gravity shifted from the inner island to the outer island). The total brightness of nighttime lights in Xiamen is gradually increasing, indicating that the level of urban economic development continuously improved over the measurement period, that human social activities have strengthened, and that the cross-island development strategy has produced certain results. These results provide data that describe urban development and policy formulation in Xiamen.

**Keywords:** nighttime light data; urban built-up area; Xiamen; urban expansion; urban center of gravity migration; intra-city differences



**Citation:** Chai, C.; He, Y.; Yu, P.; Zheng, Y.; Chen, Z.; Fan, M.; Lin, Y. Spatiotemporal Evolution Characteristics of Urbanization in the Xiamen Special Economic Zone Based on Nighttime-Light Data from 1992 to 2020. *Land* **2022**, *11*, 1264. <https://doi.org/10.3390/land11081264>

Academic Editors: Kaifang Shi, Yuanzheng Cui and Zuoqi Chen

Received: 4 July 2022

Accepted: 4 August 2022

Published: 7 August 2022

**Publisher's Note:** MDPI stays neutral with regard to jurisdictional claims in published maps and institutional affiliations.



**Copyright:** © 2022 by the authors. Licensee MDPI, Basel, Switzerland. This article is an open access article distributed under the terms and conditions of the Creative Commons Attribution (CC BY) license (<https://creativecommons.org/licenses/by/4.0/>).

## 1. Introduction

Since the reform and opening up of China, the Chinese government has promoted and achieved large-scale urbanization to accompany its continuous population growth, rapid economic development, and the concentration of non-agricultural industries in cities [1,2]. According to the data of the sixth and seventh censuses, the fraction of the urban population in China rose rapidly from 49.68% in 2010 to 63.89% in 2020, and the fraction of the urban population is still increasing by 14.21% [3]. However, the rapid growth of the urban population has been accompanied by the continuous expansion of urban land [4], which aggravates the conflicts between population, resources, and the environment [5,6]. Therefore, it is necessary to accurately understand the level of urbanization and study

the spatiotemporal evolution of urban built-up areas (UB) in China. The development of urbanization is a dynamic and complex process [7], and the traditional statistical methods based on administrative regions lack geospatial information, making it difficult to analyze and explore the regional development and spatial variations.

Remote-sensing (RS) data have become increasingly abundant as RS technology has advanced, and NTL data are now applied by numerous researchers to study urban questions. As of 2013, data from the Suomi National Polar-Orbiting Partnership Satellite's Visible Infrared Imaging Radiometer Suite (NPP/VIIRS) replaced the data of the Defense Meteorological Satellite Program's Operational Line-scan System (DMSP/OLS) because the latter suffered from discontinuities between images, image oversaturation, and difficulties updating the images. To obtain long-time sequences of NTL data, the two types of data must be calibrated and then fused. Elvidge et al. [8] proposed a correction method for invariant target regions. Sicily was selected as the invariant target region, and the F121999 NTL image was used as a reference image. The image data of other years were then compared by quadratic regression with the reference image data to obtain the corresponding quadratic regression equation. Based on these results, Liu et al. [9] selected Jixi City as the target area and corrected the Chinese DMSP/OLS images. Zou et al. [10] constructed a DMSP/OLS calibration model based on the ArcGIS platform to complete the calibration of NTL images of China. Cao et al. [11] used F162006 radiometric calibration light images as reference images to correct for over-saturated images of Hegang City, Heilongjiang province. Later, Zhang et al. [12] proposed a new index that reduces the supersaturation of DMSP/OLS images and extracts higher-spatial-resolution NTL data to observe urban centers in more detail. Wu et al. [13] constructed the normalized difference vegetation index (NDVI) to correct the saturated data, and the results show that this index alleviates the saturation of NTL data and enhances spatial heterogeneity. Xu et al. [14] proposed a compound-exponential-model-adjusted NTL index based on the vegetation-adjusted NTL urban index to better correct the oversaturation problem of images and highlight the city's internal profile and spatial heterogeneity. In addition to fitting and correcting the two types of NTL data, some researchers fuse data by using the power function model [15,16], the logarithm model [17,18], or the geographic-weighted regression model [19]. For a long time, most researchers have used the invariant target method to correct DMSP/OLS data, which improves the continuity of the data but does not address the saturation phenomenon and water overflow effects of the image data, and few studies have been reported on the fit correction with NPP/VIIRS data, which reduces the comparability of the data.

In 1978, Croft et al. [20] proposed the use of DMSP/OLS NTL data to extract UB. Later, with the improvement of NTL data, many methods were developed to extract UB, including the threshold segmentation method [21–26], the machine learning method [27–31], and the construction index method [12,32–35]. Threshold segmentation methods include the experience threshold method [21,22], the mutation detection method [23,24], the statistical data-comparison method [25], and the clustering threshold method [26]. Computer learning methods include support vector machines [27,28], artificial neural networks [29], mixed pixel linear decomposition [30], and the Sobel algorithm [31]. The constructed index method usually uses the urbanization index to extract the UB of a city, such as the enhanced UB index [32], the enhanced vegetation index (EVI)-adjusted NTL index [33], the road density and EVI-adjusted NTL index [33], the enhanced NTL index [34], and the vegetation-adjusted NTL index [12]. In addition, some researchers use logarithmic transformation to increase the difference between UB and non-urban built-up areas (NUB) and to improve the extraction of UB from NTL data [36] or fuse the RS image with higher spatial resolution to improve the extraction precision of UB [37,38].

For studying urban expansion, researchers mainly focus on the expansion speed (ES), expansion intensity (EI), expansion type, urban center of gravity, and level of development of UB [39–44]. For example, to explore the spatial and temporal variations in urbanization by county in China, Zhuo et al. [45] constructed the comprehensive-level NTL index and analyzed its correlation with urbanization by county. Based on the DMSP/OLS NTL data,

Li et al. [46] quantitatively studied the spatiotemporal evolution characteristics of urban expansion in Wuhan over the last 16 years by analyzing the spatial expansion, spatial pattern, and the migration of the urban center of gravity to provide a reference for Wuhan's urban development. Using DMSP/OLS NTL data, Mohammed et al. [47] examined the spatiotemporal evolution characteristics of Arabia's urban expansion at national and provincial levels. Rafael et al. [48] estimated the area of the global metropolitan area by calculating the urbanization rate and urban density. They also studied the distribution of city sizes by using corrected NTL data to classify light intensity. Finally, Zheng et al. [41] combined NPP/VIIRS NTL data with Landsat data to explore the spatiotemporal evolution model of urban expansion in the Guangdong–Hong Kong–Macao greater bay area (GBA).

In summary, previous studies have shown that NTL data offer unique advantages for analyzing urban questions and play a major role in urban development and planning. At present, insufficient research attention focuses on the development and variations within the Xiamen Special Economic Zone over the past 40 years; the existing research mainly discusses economy and policy, whereas few reports exist on the spatial variation of urban sprawl over time. In view of these difficulties, this paper considers the Xiamen Special Economic Zone and uses DMSP/OLS and NPP/VIIRS data as the basic data source; Landsat data, Land Use/Cover Change (LUCC) data, economic statistics data, and administrative territorial entity vector data as auxiliary data, the invariant-target method is used to correct data fusion to form a continuous, long-duration (1992–2020), and stable NTL dataset. First, the VWANUI index is used to extract UB and verify its accuracy. Second, the urban spatial pattern of Xiamen is analyzed by selecting different urban spatial expansion indicators for comparing urban development over time and space, and determining the type of urban expansion and the direction of the migration of the urban center of gravity. Next, the total amount of NTL data and the relative development rates are calculated to analyze how the inner development of Xiamen city differs from the relative development rate of each district. Finally, the driving factors of urban expansion are discussed, and some suggestions and strategies for optimization are put forward. It is of great significance to the research on the expansion of Xiamen from an island-based to a bay-based city. The results provide data that describe urban development, which allows for an objective analysis of government policy.

## 2. Materials and Methods

### 2.1. Study Area

Xiamen, located in the southeast of Fujian Province, is an important central city, seaport, and scenic tourist city on the southeast coast of China. Siming, Huli, Jimei, Haicang, Tong'an, and Xiang'an are the city's administrative districts. The city has a land area of 1700.61 km<sup>2</sup> and a sea area of almost 390 km<sup>2</sup> (Figure 1). At the end of 2020, Xiamen had a permanent population of 5.164 million [49]. In 2021, Xiamen's gross domestic product (GDP) reached RMB 703.389 billion [50].

Xiamen's unique geographical location makes it stand apart from cities on land. The island is a typical island city, while the outer islands show the characteristics of a mountainous city [51]. In the process of urbanization, the surrounding sea area has limited the expansion of the city to a certain extent, and the early urban development was mainly concentrated on the island, resulting in an extreme imbalance between the development inside and outside the island, with data showing that in 2000, the resident population density inside the island was more than 10 times that outside the island [52]. As a result, Xiamen was faced with the problem of optimizing intra-urban development earlier than other plain cities, which makes the study of the evolution of urbanization in Xiamen more special and necessary.

Xiamen is one of the earliest special economic zones in China and is the fastest growing and most dynamic economic region in the coastal region. For 40 years, with the support of its designation as a "Special Economic Zone", Xiamen underwent strong economic development while retaining a beautiful ecological environment through the "Xiamen Speed" program [53]. In 2002, Xi Jinping, then governor of Fujian Province, proposed

the “cross-island development” strategy for Xiamen [54]. Visually quantifying the spatial expansion and balancing the development of Xiamen since the establishment of the Xiamen Special Economic Zone and the cross-island development strategy have been critical to better coordinating regional development.

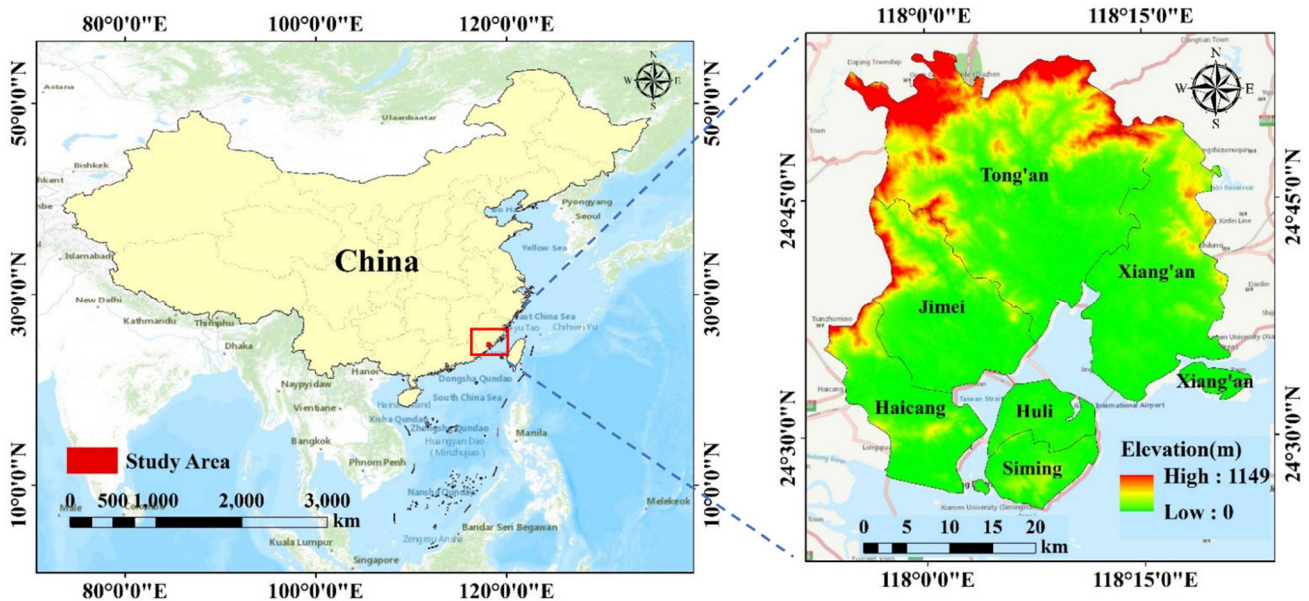


Figure 1. Location of study area.

## 2.2. Data Source and Processing

### 2.2.1. Data Source

#### (1) NTL data

The DMSP/OLS NTL data are from the National Oceanic & Atmospheric Administration’s National Geophysical Data Center (NOAA/NGDC) and were acquired by the weather satellite’s operational infrared scanning sensor (OLS). The NTL data source contains 34 images acquired over 22 years, covering the period 1992–2013. The digital number (DN) range is 0–63, the spatial resolution is 1000 m, the reference frame is WGS-84, and accidental noise such as clouds and firelight has been filtered out. It is worth noting that despite the disadvantages of oversaturation and spillover effects, because of the abundance of archived data, long time span, and wide spatial coverage, the DMSP/OLS NTL data are widely used to study urban sprawl, socio-economic estimates, ecology, fisheries, and so on [55].

The NPP/VIIRS NTL data were provided by the NOAA/NGDC and detected by the VIIRS onboard the NPP. Its image includes monthly data and annual data. The monthly data, which began to be available in April 2012 and are now updated to 2021, filter out the effects of lightning, moonlight, and cloud cover, but other transient light and background noises, such as auroras, flares, and ships, are not filtered [55]. Compared with DMSP/OLS NTL data, NPP/VIIRS data not only inherit the basic characteristics of DMSP/OLS data but also offer improved spatial resolution, which can be as high as 500 m, and solve the oversaturation of DMSP/OLS data.

#### (2) Other data

The Landsat data used herein are derived from a Geospatial Data Cloud, and the LUCC data are derived from the Resource and Environment Science and Data Center. The statistics data come from the yearbook of the Xiamen Special Economic Zone. The administrative division data are based on a 1:4 million national database provided by the National Geographic Center of China.

### 2.2.2. Data Processing

#### (1) Data correction

Based on the research results of Elvidge et al. [8] and Liu et al. [9] and given its relatively stable urban development, this study uses the city of Jixi as the target invariant region. The 34 stable NTL images and the F162007 images with better continuity and higher gray values were then used as corrected images and reference images, respectively, and their  $DN$ s were calculated by quadratic regression:

$$DN_c = a \times DN^2 + b \times DN + c \tag{1}$$

where  $DN$  is the initial  $DN$  value,  $DN_c$  is the corrected  $DN$  value, and  $a$ ,  $b$ , and  $c$  are coefficients.

The NTL data of a given year are acquired independently by different sensors. To address the discontinuity between the corrected images, the corrected dataset requires an intra-annual composition, which is expressed as [9]:

$$DN_{(n,i)} = \begin{cases} 0 & DN_{(n,i)}^x = 0, DN_{(n,i)}^y = 0 \\ (DN_{(n,i)}^x + DN_{(n,i)}^y) / 2 & \text{otherwise} \end{cases} \tag{2}$$

where  $DN_{(n,i)}^x$  and  $DN_{(n,i)}^y$  are the  $DN$  values of pixel  $i$  obtained by two different sensors in year  $n$  after calibration,  $DN_{(n,i)}$  is the  $DN$  value of pixel  $i$  in year  $n$  after images' intra-annual composition, and  $n = 1994, 1997, 1998, \dots, 2007$ .

After the intra-annual composite, incomparable images remained between different years, so the following inter-annual series correction was applied [9]:

$$DN_{(n,i)} = \begin{cases} 0 & DN_{(n+1,i)} = 0 \\ DN_{(n-1,i)} & DN_{(n+1,i)} > 0 \cap DN_{(n-1,i)} > DN_{(n,i)} \\ DN_{(n,i)} & \text{otherwise} \end{cases} \tag{3}$$

where  $DN_{(n-1,i)}$ ,  $DN_{(n,i)}$ ,  $DN_{(n+1,i)}$ , are the  $DN$  values of pixel  $i$  in year  $n - 1$ ,  $n$ , and  $n + 1$  after image correction, respectively, and  $n = 1992, 1993, \dots, 2013$ .

#### (2) Data fusion

Although the NPP/VIIRS monthly data are free of the effects of lightning, moonlight, and cloud cover, transient-light sources such as aurora, firelight, and background noise were not removed. In this paper, the October image of each year of NPP/VIIRS images serves to represent the given year. First, the NPP/VIIRS images are subjected to preprocessing (reprojection, resampling, cropping, depolarization, and denoising) to obtain stable NTL data. Next, the NPP/VIIRS images are converted to the DMSP/OLS image range scale by using the target-invariant method, the DMSP/OLS images from 2012 and the logarithmic NPP/VIIRS images from 2013 to 2020 are linearly regressed, and the regression model with the highest correlation is chosen to complete the correction of NPP/VIIRS data as follows:

$$DN_c = a \times (LgDN)^2 + b \times LgDN + c \tag{4}$$

where  $LgDN$  is the initial  $DN$  value of the logarithmic NPP/VIIRS images,  $DN_c$  is the corrected  $DN$  value, and  $a$ ,  $b$ , and  $c$  are regression coefficients. Equation (3) above gives the interannual continuity correction of the image data.

#### (3) Evaluation of correction results

The DMSP/OLS and NPP/VIIRS data are corrected and fused in this study, Figure 2 shows some of the correction results.

The total  $DN$ s of the long-time-sequence NTL data from 1992 to 2020 in Xiamen were analyzed by the above-mentioned correction procedure. Figure 3 shows that the two types of NTL data are fused by the fitting correction, and the image data are unique every year. There are no abnormal fluctuations, but a stable and increasing trend appears. The

long-time sequence of NTL data with stability and continuity is formed, and the corrected results are accurate.

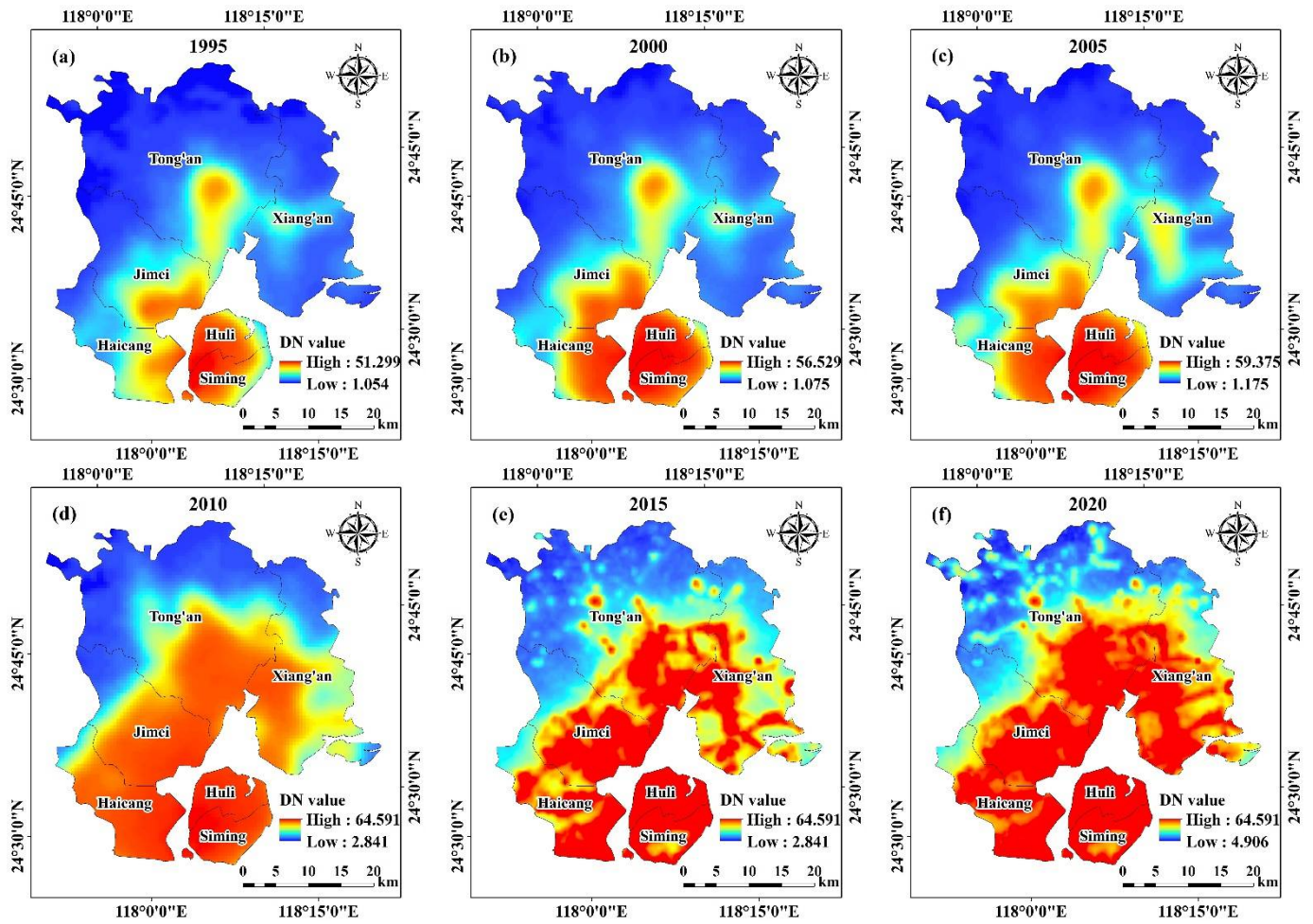


Figure 2. Results of partial image correction for Xiamen: (a) 1995 NTL, (b) 2000 NTL, (c) 2005 NTL, (d) 2010 NTL, (e) 2015 NTL, (f) 2020 NTL.

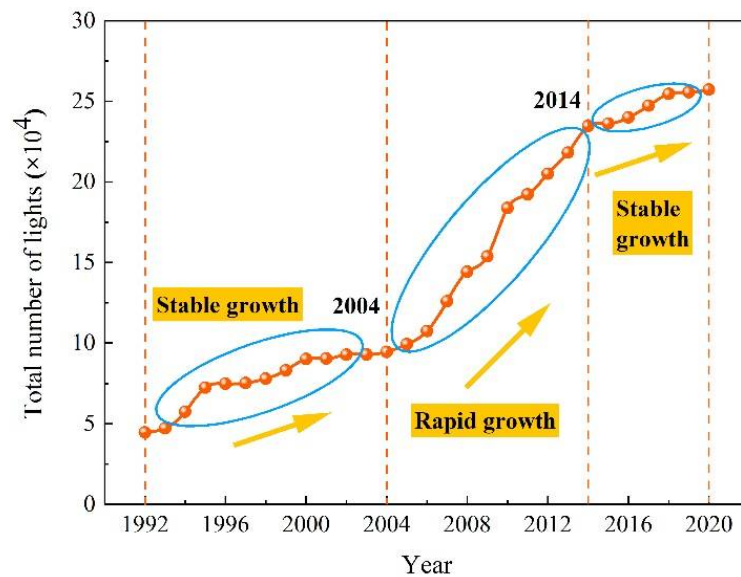


Figure 3. Total DN values from NTL images of Xiamen for the period 1992–2020.

As can be seen from Figure 3, the growth in NTL was more stable in the period 1992–2005, more rapid in the period 2005–2014, and gradually stabilized in the period 2014–2020. This result is explained by the dramatic growth of the economy and society. The noctilucous image of the city center in the middle and late phases of the city’s development shows stable pixels and continuously expands outwards from the city center. At the same time, the implementation of the strategy of cross-island development promoted the cross-island flow of talent and industries, expanded the development space inside and outside the island, and promoted the economic development of Xiamen.

The results reveal a high correlation between NTL and GDP [56,57]. This work applies a regression analysis of the total number of lights (TNL) and of the GDP for the long-time sequence NTL images of Xiamen from 1992 to 2020 before and after the correction (Table 1). The results indicate that the goodness-of-fit  $R^2$  of the regression model before and after correction is greater than 0.89, and the  $p$ -value is less than 0.01. Again, a strong correlation exists between total DN and GDP. The  $R^2$  of the corrected regression model is greater than before correction and greater than 0.91, and the  $p$ -value is less than before correction, which is indicative of the improved results from data correction. The problems of data discontinuity, spillover effects, and supersaturation are weakened or eliminated, reflecting the social and economic activities.

**Table 1.** Parameters of linear regression models of TNL and GDP.

Linear Regression Parameter	Before Correction	After Correction
Regression model	$y = 0.0745x - 2138.8$	$y = 37.527x + 69,963$
$R^2$	0.8963	0.9152
$p$ -value (intercept)	$7.85 \times 10^{-18}$	$1.98 \times 10^{-12}$
$p$ -value ( $x$ variable)	$9.22 \times 10^{-15}$	$1.56 \times 10^{-16}$

### 2.3. Extraction of UB

To effectively extract the UB of the city, firstly, based on the study of Zheng et al. [58], this paper uses Landsat remote-sensing images to obtain the NDVI and the normalized difference water index (NDWI) to construct the VWANUI. Secondly, the dichotomous method [24,59] is used to obtain the potential thresholds, and LUCC is selected as the reference data to determine the best extraction threshold. Finally, the accuracy of the results was assessed using a confusion matrix. The VWANUI is calculated as follows:

$$VWANUI = Lg(NTL) \times (1 - NDVI) \times NDWI_a \quad (5)$$

$$NDVI = \frac{NIR - R}{NIR + R} \quad (6)$$

$$NDWI = \frac{G - NIR}{G + NIR} \quad (7)$$

$$-1 \leq NDWI \leq 1 \quad (8)$$

$$NDWI_a = \begin{cases} 1, & NDWI < 0.1 \\ 0, & NDWI > 0.1 \end{cases} \quad (9)$$

where  $NTL$  denotes the NTL DN value,  $NIR$  denotes the near-infrared band,  $R$  denotes the red band, and  $G$  denotes the green band.

To accurately assess the results of the UB extraction, we have selected LUCC data as basic reference data. The accuracy and reliability of the extracted results are quantified by calculating the producer’s accuracy (PA), user’s accuracy (UA), F-score, overall accuracy (OA), and kappa coefficients. We construct the confusion matrix as per the study of Shao et al. [60,61] (see Table 2). The PA represents the probability that the reference data is correctly classified, and the UA represents the probability that the points falling in the category are correctly classified. The calculations are given in Table 2.

**Table 2.** Confusion matrix.

Map Data	Reference Data			Map Total	UA
	$j = 1$	$j = 2$	$j = J$		
$i = 1$	$n_{11}$	$n_{12}$	$n_{1J}$	$n_{1+}$	$n_{11}/n_{1+}$
$i = 2$	$n_{21}$	$n_{22}$	$n_{2J}$	$n_{2+}$	$n_{22}/n_{2+}$
$i = J$	$n_{J1}$	$n_{J2}$	$n_{JJ}$	$n_{J+}$	$n_{JJ}/n_{J+}$
Reference total	$n_1$	$n_2$	$n_J$	$N$	
PA	$n_{11}/n_1$	$n_{22}/n_2$	$n_{JJ}/n_J$		

In addition, the F-score, OA, and kappa are computed based on the confusion matrix as follows:

$$F - \text{score} = 2 \times (PA \times UA) / (PA + UA) \tag{10}$$

$$OA = \frac{\sum_{j=1}^J n_{jj}}{N} \tag{11}$$

$$kappa = \frac{N \sum_{j=1}^J n_{jj} - \sum_{j=1}^J (n_j n_{j+})}{N^2 - \sum_{j=1}^J (n_j n_{j+})} \tag{12}$$

where  $N$  denotes the total number of categorical points,  $n_{jj}$  is the diagonal elements of the error matrix,  $n_j$  is the column sum of categories, and  $n_{j+}$  is the row sum of categories.

#### 2.4. Study of Expansion Pattern of UB

To analyze the changes in the expansion of Xiamen’s UB from 1995 to 2020, we use the ES (km<sup>2</sup>/year) [62] and EI (%) [63] to quantify the expansion of UB. The ES is the average annual expansion of UB over a certain time. However, it is extremely hard to quantify urban expansion, so EI is introduced to reflect the strengths and weaknesses of UB expansion during the study period. The ES and EI are calculated as follows:

$$ES = \frac{A_m - A_c}{T} \tag{13}$$

$$EI = \frac{ES}{A} \times 100\% \tag{14}$$

where  $A_c$  denotes the initial UB,  $A_m$  denotes the final UB,  $A$  denotes the total area, and  $T$  denotes a time period.

#### 2.5. Study of the Migration of the Center of Gravity within UB

The urban center of gravity is a key index for describing a city’s spatial distribution, which can be thought of as the city’s average position and the equilibrium point for the city to maintain a uniform distribution [64]. Calculating the spatial urban center of gravity of UB helps to quantitatively analyze the variations in urban expansion. The formula is calculated as follows:

$$X = \frac{\sum_{i=1}^n (C_i \times x_i)}{\sum_{i=1}^n C_i}; Y = \frac{\sum_{i=1}^n (C_i \times y_i)}{\sum_{i=1}^n C_i} \tag{15}$$

where  $X$  and  $Y$  denote the horizontal and vertical coordinates of the urban center of gravity,  $C_i$  denotes the area of UB of a small area  $i$ , and  $x_i, y_i$  denote the horizontal and vertical coordinates of the geometric center of the small area  $i$ .

In this paper, the law of the migration of the urban center of gravity is studied via three indexes: migration distance, migration velocity, and migration angle. These quantities are calculated as follows:

$$D_c = \sqrt{(x_c - x_{c-1})^2 + (y_c - y_{c-1})^2} \tag{16}$$



$$V_c = \frac{D_c}{T} \quad (17)$$

$$\theta_c = n\pi + \operatorname{atan}\left(\frac{y_c - y_{c-1}}{x_c - x_{c-1}}\right) \quad (n = 0, 1, 2) \quad (18)$$

where  $x_c$  and  $y_c$  denote the horizontal and vertical coordinates of the urban center of gravity in year  $c$ ,  $x_{c-1}$  and  $y_{c-1}$  denote the horizontal and vertical coordinates in year  $c - 1$ , and  $T$  denotes a time period.

## 2.6. Study of Differences in Intra-City Development

### 2.6.1. Differences in Intracity Development

This paper studies the six urban districts of Xiamen and calculates the TNL to characterize the development of the cities. The overall differences in intra-city development are quantified by the standard deviation (SD) and coefficient of variation (CV) [65], which are calculated as follows:

$$TNL = \sum_{i=1}^n (DN_i \times C_i) \quad (19)$$

$$SD = \sqrt{\frac{\sum_{i=1}^n (TNL_i - TNL_m)^2}{n}} \quad (20)$$

$$CV = \frac{SD}{TNL} \quad (21)$$

where  $DN_i$  is the  $i$ th level gray value,  $C_i$  is the number of grids of level  $i$  of the gray value,  $n$  is the number of urban districts,  $TNL_i$  is the total number of lights in urban district  $i$ , and  $TNL_m$  is the mean value of lights of urban district  $m$ . The larger the CV, the more concentrated is the city's development and, conversely, the smaller the CV, the more dispersed is the city's development.

### 2.6.2. Relative Development within the City

The relative development rate (RDR) [66] is the ratio of the level of development of a district over a certain period to the level of development of the whole city during the same period. It is calculated as follows:

$$RDR = \frac{TNL_{mi} - TNL_{ci}}{TNL_m - TNL_c} \quad (22)$$

where  $TNL_{ci}$  and  $TNL_{mi}$  are the total lights in urban district  $i$  at the beginning and end of the study period, and  $TNL_1$  and  $TNL_2$  are the total lights of the city as a whole at the beginning and end of the study period.

## 3. Results

### 3.1. Analysis of Extraction Results from UB

In this work, we use the LUCC data of Xiamen city as reference data and divide them into two types, UB and NUB, following which, the accuracy of the extracted UB is verified. The VWANUI index (i) reduces the oversaturation of the noctiluent image of the city center, (ii) removes the overspill effect of the noctiluent image in the vegetation and water area, and (iii) enhances the variability in the urban area. We take the 2010 NTL image, shown in Figure 4, and combine it with the dichotomy to extract the UB of Xiamen in 1995, 2000, 2005, 2010, 2015, and 2020 (Figure 5). The accuracy evaluation metrics PA, UA, F-score, OA, and Kappa coefficients were calculated by the confusion matrix (Table 3). These results show that as the accuracy of the VWANUI increases, the F-score is over 74%, the OA exceeds 90%, and the kappa coefficient exceeds 70%, which means that the urban information extracted in this work is suitable for research into urban spatial change.

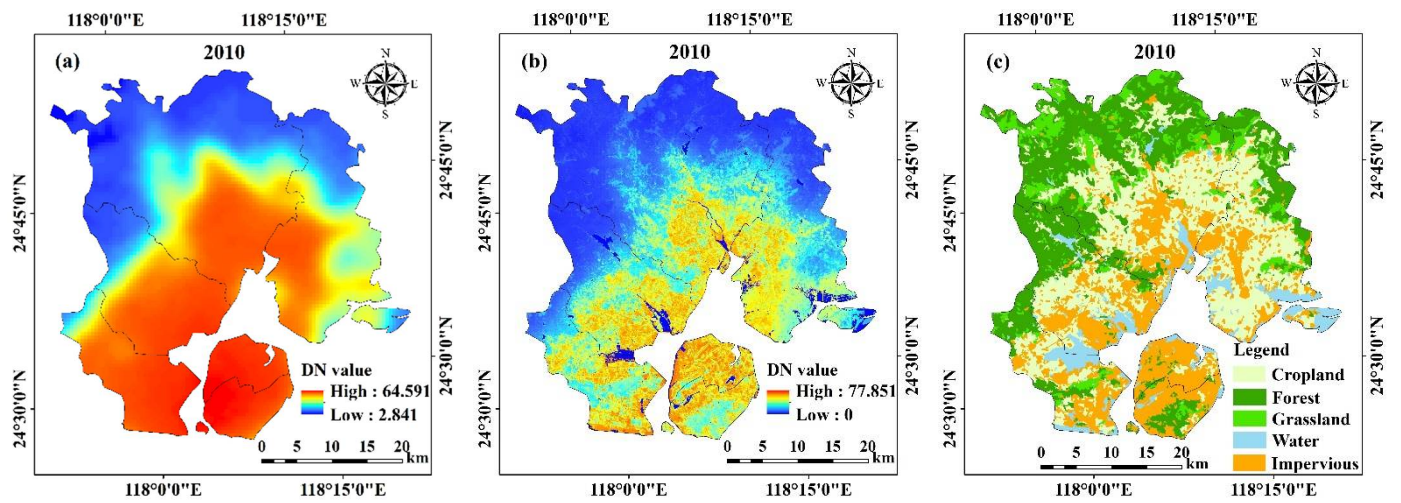


Figure 4. Comparison of 2010 (a) NTL, (b) VWANUI, and (c) LUCC in Xiamen.

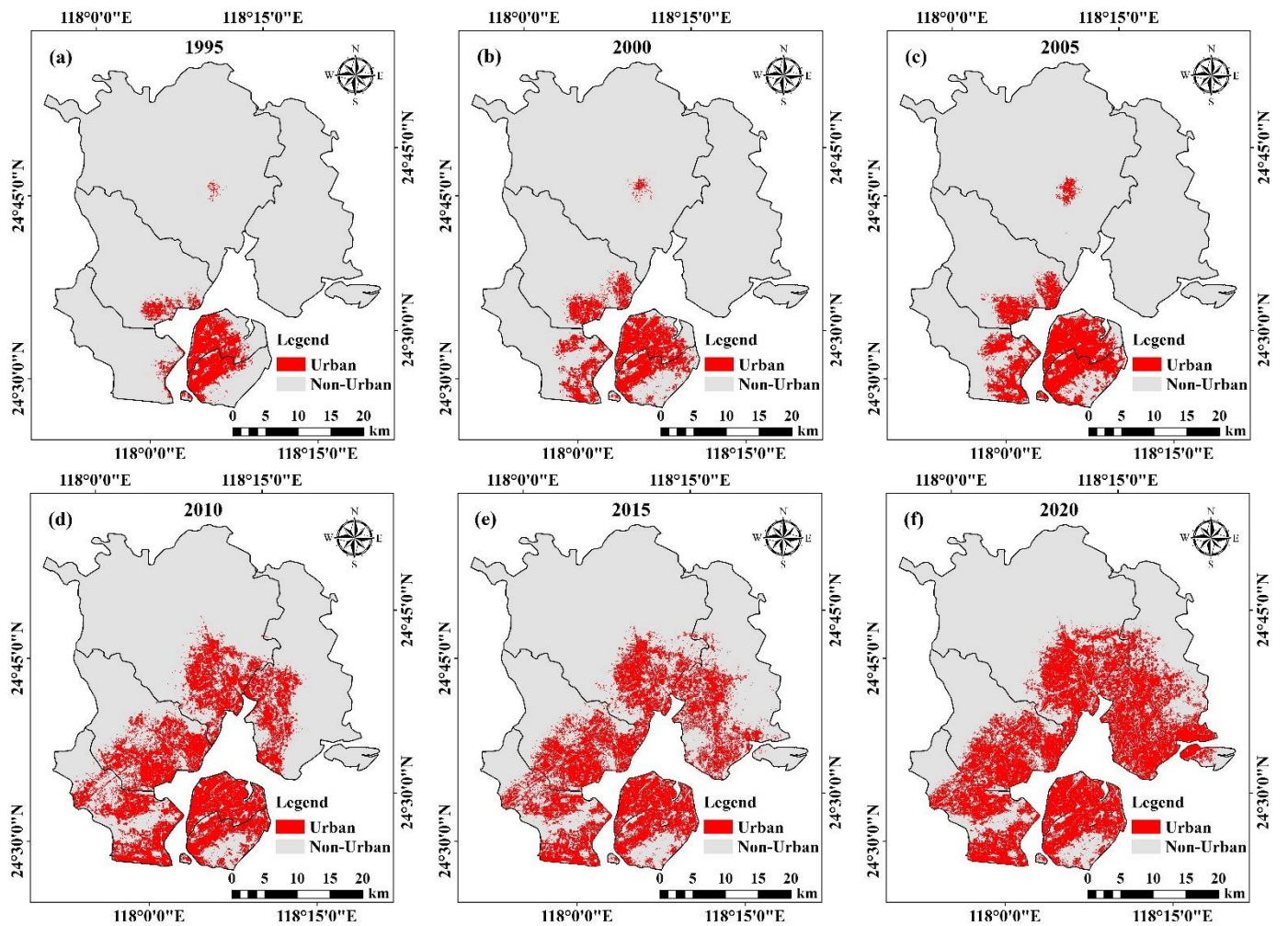


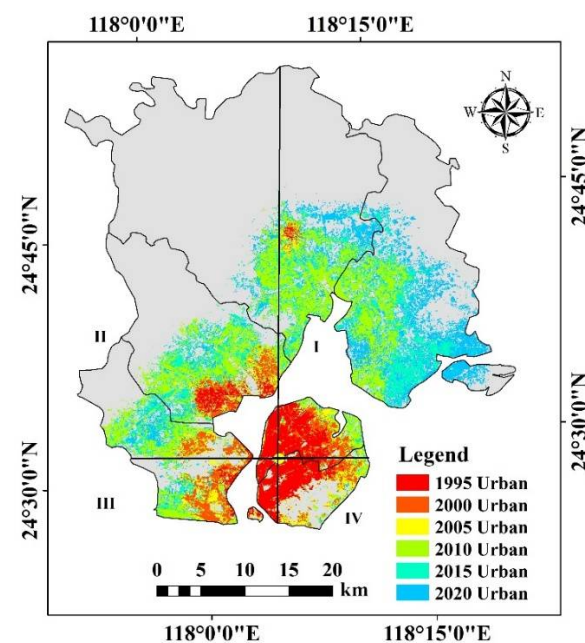
Figure 5. Extraction of UB in Xiamen from 1995 to 2020. (a) 1995 UB, (b) 2000 UB, (c) 2005 UB, (d) 2010 UB, (e) 2015 UB (f) 2020 UB.

**Table 3.** Accuracy evaluation index table of UB extraction.

Year	PA	UA	F-Score	OA	Kappa
1995	69.57%	80.38%	74.59%	97.93%	73.51%
2000	75.51%	72.70%	74.08%	97.33%	72.67%
2005	72.13%	79.47%	75.62%	96.02%	73.46%
2010	70.43%	85.94%	77.42%	92.51%	72.98%
2015	80.79%	78.76%	79.76%	91.96%	74.75%
2020	80.29%	83.46%	81.85%	90.16%	75.09%

### 3.2. Analysis of Expansion Pattern of UB

To accurately analyze the expansion of Xiamen's UB, we divide Xiamen city into four quadrants by superimposing the urban built-up areas in 1995, 2000, 2005, 2010, 2015, and 2020, and establishing a coordinate system with the urban center in 1995 as the coordinate origin and east as the positive direction of the horizontal axis, as shown in Figure 6. Table 4 gives the calculated results of the expansion of Xiamen for each phase of the study phase.

**Figure 6.** Expansion of UB in Xiamen from 1992 to 2020.**Table 4.** Expansion of Xiamen's UB at different phases of the study.

Type	Phase I 1995–2000	Phase II 2000–2005	Phase III 2005–2010	Phase IV 2010–2015	Phase V 2015–2020	Study Phase 1995–2020
Expansion area (km <sup>2</sup> )	28.620	43.190	112.170	61.123	104.116	349.219
Expansion speed (km <sup>2</sup> /year)	5.724	8.638	22.434	12.225	20.823	13.968
Expansion intensity (%)	0.337	0.508	1.319	0.719	1.225	0.821
Expansion contribution rate (%)	8.194	12.368	32.120	17.503	29.814	100.000

In general, the urban spatial expansion of Xiamen from 1995 to 2020 was mainly island-centered and outward-oriented. During the period 1995–2005, the urban expansion of Xiamen was subtle, the expansion was mainly directed westward, with a slight increase in other directions, and the urban expansion was slow.

During the period 2005–2010, the expansion was mainly towards the north and southwest, with almost no change to the southeast. The largest expansion was in this phase, accounting for about 33% of the total expansion. The expansion speed, intensity, and contribution rate were also the largest in this area. This reflects the accelerated expansion

of the city in this phase, which was mainly due to the saturated development space in the southeast. No potential for marginal expansion was available, and expansion in other directions may be due to the development and construction of the southern Haicang and Xinglin Maluan Bay around the western sea. Another contribution to the development was the improvement of urban functions such as in the satellite cities of Jimei, Xiang'an, and Tong'an. These improvements strongly promoted social and economic activities in these areas and accelerated their urbanization.

During the period 2010–2015, urban expansion was mainly directed to the northwest and northeast due to the island's focus on promoting the development and transformation of urban villages such as the cross-strait financial center area and the Wuyuan Bay area, and on promoting the construction of Jimei New Town off the island, which gradually improved the housing conditions and living environment of residents and raised the level of the area's infrastructure and public service facilities. At the same time, this result also reflects the gradual transformation of Xiamen from an island-based to a bay-based city.

During the period 2015–2020, urban expansion mainly occurred in the northwest and northeast directions. This was the result of the comprehensive development of Xinglin Bay Business Operation Center, Software Park III, Tong'an New Town, and Xiang'an New Town. The continuous improvement of medical services, embodied by the Maluan Bay Hospital and East Sea Area Hospital, and the rapid development of transportation infrastructure such as Xiang'an Bridge, the Fuzhou–Xiamen high-speed railway, and the Xiang'an International Airport. All these factors contributed to accelerating urbanization.

In addition, the expansion of the UB in the third–fifth phases accounted for 79.44% of the total study period. Therefore, Xiamen's urban expansion is mainly concentrated in the period 2005–2020. Combining this result with Figure 6, we further conclude that the urban expansion in this study phase extended from the island (Siming, Huli) to beyond the island (Haicang, Jimei, Xiang'an, Tong'an) [42], which is an important reflection of the effectiveness of Xiamen's cross-island development strategy.

### 3.3. Analysis of the Migration of the Urban Center of Gravity

In this paper, the location of the urban center of gravity and the migration route of Xiamen's urban built-up area from 1995 to 2020 are calculated according to the formula for the migration of the urban center of gravity (see Figure 7). The results are given in Table 5.

As shown in Figure 7 and Table 5, from 1995 to 2000, the urban center of gravity of the UB of Xiamen moved 923.52 m to 53.41° southwest. From 2000 to 2005, the urban center of gravity of the UB of Xiamen moved 628.23 m to the northeast, with a migration angle of 86.70° to the northeast. From 2005 to 2010, the urban center of gravity of the UB of Xiamen continued to move 6600.03 m to the northeast, for an annual migration as high as 1320.01 m/year. From 2010 to 2015, the urban center of gravity of the UB of Xiamen moved 759.06 m at the speed of 151.81 m/year in the direction of 60.02° to the northeast. From 2015 to 2020, the urban center of gravity of the UB of Xiamen moved 2380.21 m in the direction of 53.83° northeast.

During the period of 1995–2000 and 2000–2005, the urban center of gravity of the UB of Xiamen city shifted, although it remained basically on the island of Xiamen. This is because the spatial layout of Xiamen was too concentrated on the island and the island was overdeveloped. This forced a rapid development of the inner area until saturation gradually set in.

From 2005 to 2010, the urban center of gravity of the UB of Xiamen city shifted from the island to the outer island, with the fastest rate of the urban center of gravity's shift being mainly because Xi Jinping, then governor of Fujian Province, proposed the cross-island development strategy for Xiamen in 2002. The cross-island extension of public services such as health care, education, and transportation facilitated the cross-island migration of the urban center of gravity of the city.

In 2010–2015 and 2015–2020, the city's center of gravity shifted to the northeast, which was the result of the Xiamen City Urban Master Plan (2011–2020). Xiamen proposed to

form “one island, one belt, and multiple centers” as a cluster-type bay–city pattern. The optimization of Xiamen island led to the large-scale development and construction of such areas as Haicang New Town, Jimei New Town, Tong’an New Town, and Xiang’an New Town outside the island, and to the improvement of public facilities and infrastructure. Xiamen also accelerated urbanization, resulting in the economy of the bay city becoming the largest growth pole for the future development of Xiamen.

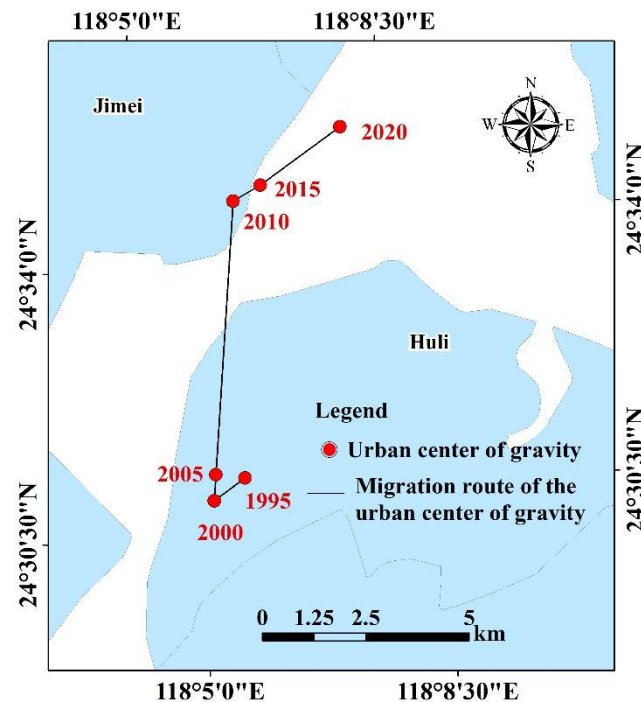


**Figure 7.** Location and migration route of the urban center of gravity in Xiamen.

**Table 5.** Results of the migration of the urban center of gravity in Xiamen.

Year	Migration Distance (m)	Migration Speed (m/year)	Migration Angle (Degrees)
1995–2000	923.52	184.70	Southwest 53.41°
2000–2005	628.23	125.65	Northeast 86.70°
2005–2010	6600.03	1320.01	Northeast 86.40°
2010–2015	759.06	151.81	East-north 60.02°
2015–2020	2380.21	476.04	East-north 53.83°
1995–2020	8757.15	350.29	Northeast 74.88°

In general, from 1995 to 2020, the urban center of gravity of the UB of Xiamen shifted 8757.15 m in the direction of 74.88° northeast, which translates into a migration speed of 350.29 m/year. Xiamen’s urban development continued to move in the north-northeast direction throughout the study period, continuously promoting coordinated regional development and narrowing the gap between on- and off-island. According to the results of Zhan et al. [67], the urban center of gravity of Xiamen city shifted north from 2000 to 2013, moving from the inner island to the outer island. The results of the present work are consistent with those of Zhan et al., which is indicative of their accuracy and reliability.

### 3.4. Analysis of Variations in Intra-City Development

#### 3.4.1. Analysis of Variations in Urban Development

To understand the differences in the internal development of each district in Xiamen, we calculate the DN of the total number of lights and the differences among districts in Xiamen. Table 6 gives the results.

**Table 6.** Total number and differences of lighting DN for districts in Xiamen.

City District	Total Number of Lights in Each District of Xiamen					
	1995	2000	2005	2010	2015	2020
Siming	9147.25	11,429.47	12,236.55	13,417.43	15,644.09	15,735.82
Huli	9471.22	11,498.32	12,032.67	13,683.39	16,555.98	16,565.98
Haicang	11,454.28	16,431.84	18,075.49	28,413.13	33,295.08	34,538.67
Jimei	14,184.38	17,474.29	18,129.42	33,351.99	41,682.25	43,563.67
Tong'an	18,296.26	21,430.37	22,385.11	53,247.78	71,690.61	83,531.76
Xiang'an	19,894.74	21,872.44	22,907.88	41,616.64	57,327.99	63,330.82
TNL	82,448.13	100,136.73	105,767.12	183,730.37	236,196.01	257,266.73
Mean	13,741.35	16,689.46	17,627.85	30,621.73	39,366.00	42,877.79
SD	4150.87	4176.07	4307.64	14,306.49	20,382.84	24,392.90
CV	0.30	0.25	0.24	0.47	0.52	0.57

Figure 8 shows the total number of lights in each district of Xiamen city as a function of time. The results show that the total number of lights in each district of Xiamen city experienced different growth rates over time, indicating an increasing rate of development. The growth of Siming District and Huli District on the island remained more constant, which may be attributed to the island's smaller size and relatively balanced socio-economic development. The TNL in the off-island area increased significantly, especially in Tong'an and Xiang'an, showing a trend of high growth since 2010, which is attributed to the launch of the integrated development strategy of Xiamen on and off the island in 2010. This caused Xiamen's urban construction to shift from on the island to off the island, accelerating the development of new towns and industrial zones off the island, improving the area's medical facilities and public facilities, strengthening the connection between the island and outside the island, and driving the development of the city.

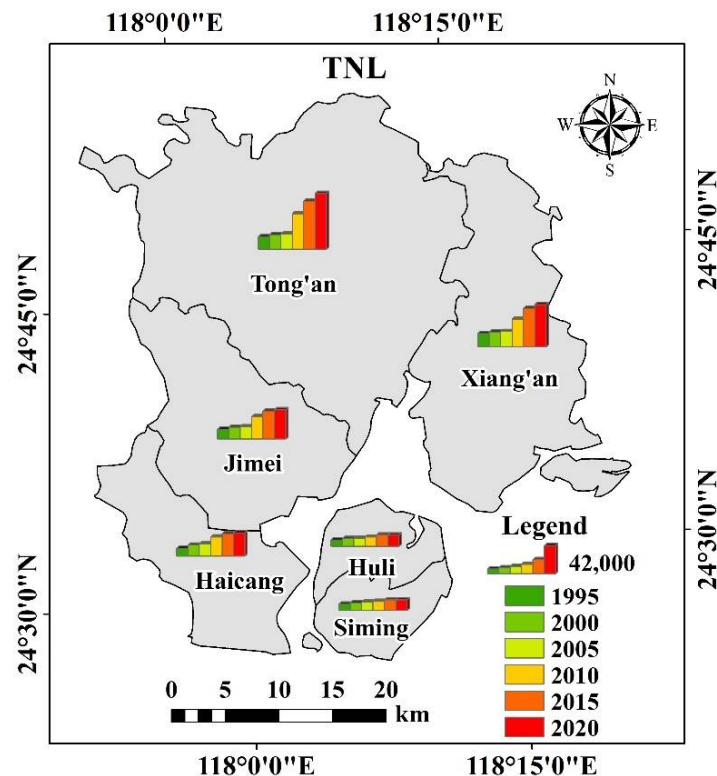


**Figure 8.** Total number of lights of districts in Xiamen.

Figure 9 shows the total number of lights, the mean number of lights, and the coefficient of variation of Xiamen city as functions of time. The results show that the total number

of lights and their mean number in Xiamen gradually increased over time, reflecting the increasing development of the city over time. Since 2005, the coefficient of variation has gradually increased, indicating an increasing concentration of the development of cities.

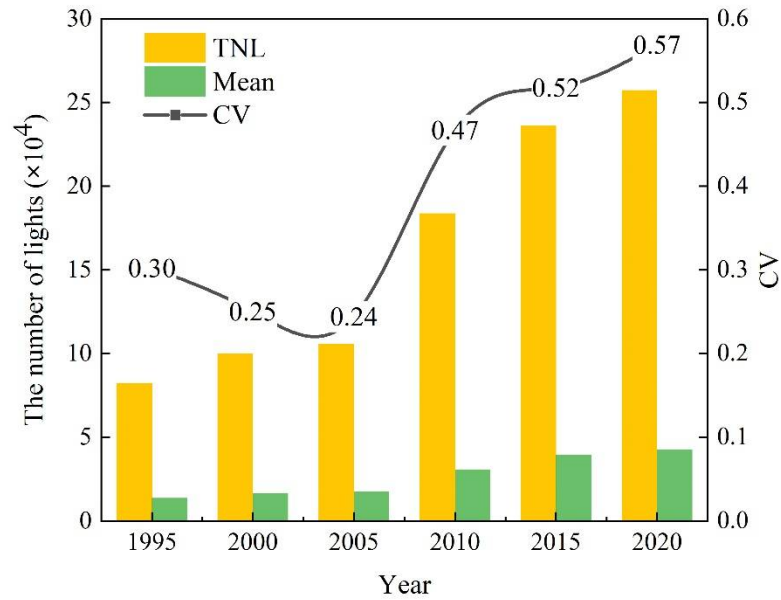


Figure 9. TNL, mean, and CV in Xiamen.

### 3.4.2. Analysis of the RDR

The relative rate of development of each district in Xiamen at different stages was calculated, and the results are shown in Figure 10.

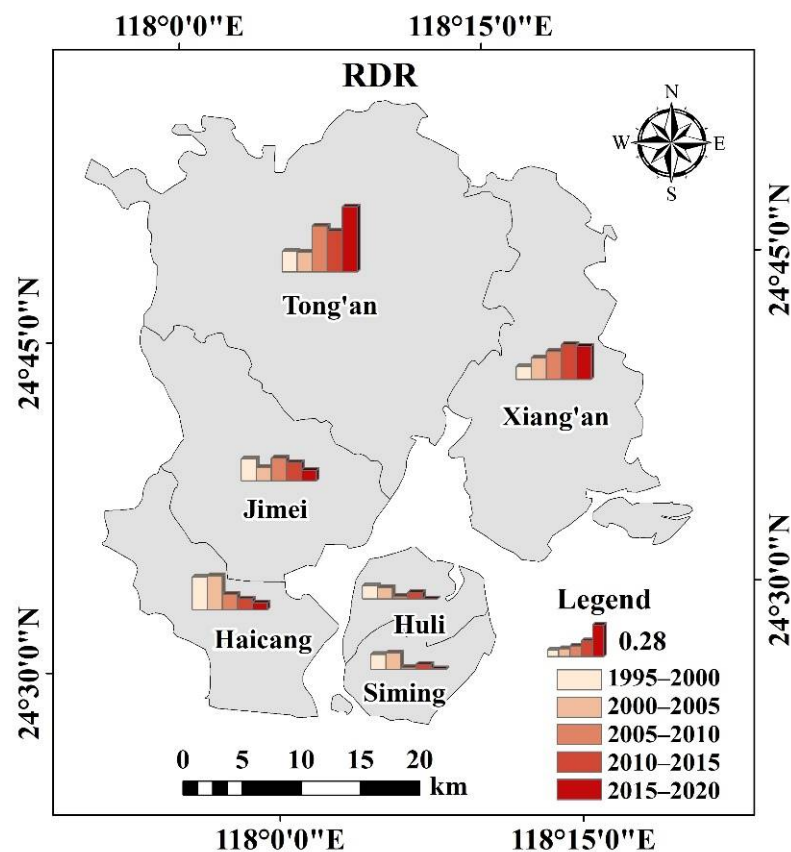


Figure 10. Comparison of RDR at different phases and in the different districts of Xiamen.

As shown by Figure 10, the relative rates of development of Siming district and Huli district (on Xiamen island) decrease monotonically over time, especially in the period 2005–2020, when the relative development rate of these cities is close to zero, which indicates that the development of Siming and Huli districts was close to saturation during this phase. The urban development that was centered on the island gradually expanded to the regions off the island. The relative development rates of Haicang and Jimei districts decreased as of the third phase (2005–2010), indicating that their development gradually slowed and saturated. In contrast, the relative rate of development of Tong'an and Xiang'an districts gradually increased, indicating that the government was investing more and more in their development, reflecting the pivotal role of national policies in urbanization development.

## 4. Discussion

### 4.1. Driving Force Analysis

Urban expansion is closely related to driving factors such as physical geography, population, GDP, and policy. This study shows that Xiamen experienced rapid urban expansion between 1995 and 2020, with an expansion area of 349.219 km<sup>2</sup>, and the urban expansion was mainly concentrated in the period 2005–2020 (Figure 6 and Table 4). Policy is one of the main drivers of urban expansion and is strongly responsible for this result. Previous studies have shown that urban expansion is closely related to urban planning and related policies [62,68]. As a special economic zone, Xiamen has obvious advantages in terms of resources. However, due to its special geographic location, the development on and off the island is unbalanced, and the development of the island is basically saturated. The development off the island lags, which aggravates the gap between the on- and off-island parts. For example, in 2000, the resident population on the island was about 1.096 million, accounting for 53.4% of the city's total population, making for a population density of about 6951 persons per square kilometer and an off-island population density of about 620 persons per square kilometer. The population density on the island was over 10 times that off the island [52]. In 2002, Xiamen's "cross-island development" strategy was introduced, and the local government accelerated the implementation of the "combination of upgrading the island and expanding the bay," promoting the expansion of the city's spatial pattern, layout optimization, and functional improvement. In addition, throughout the study period, Xiamen's urban development continued to move toward the north and northeast, with the urban center of gravity shifting from the island to the outer islands (Figure 7), a result that was influenced by factors such as population, GDP, and policy. With the increase in population, rapid socio-economic development, and the implementation of relevant policies, the industrial structure of the intra-island area has been optimized. In addition, the rapid rise of large-scale townships off the island and the improvement of public facilities and infrastructure facilities have accelerated the formation of a grouped bay city pattern and promoted urbanization in Xiamen.

Upon comparing the changes in TNL by district (Figure 8), a strong correlation appears between TNL and urban expansion. As the island of Xiamen covers a relatively small area of approximately 157.76 km<sup>2</sup>, this factor has limited the urban expansion of the island. In addition, significant talents and capital have gathered on the island, contributing to the early development of the island region. Therefore, the TNL on the island has slowly increased, early urban development tends to be saturated, and urban expansion is limited. However, guided by the cross-island development strategy and the integrated development strategy of Xiamen's inner and outer islands, the construction of transport infrastructure and the improvement of medical and public facilities off the islands have been accelerated. The result is that more enterprises and citizens now congregate off the islands. A total of 3.193 million people live outside the islands as of 2021, accounting for 60.5% of the city's population, up from 46.6% in 2002 [69]. As a result, the TNL in the off-island area increased significantly, as did the off-island area's ability to expand. Previous studies have shown that population and GDP can contribute significantly to urban expansion [70,71], which is also supported by this work.



With population growth and the acceleration of urbanization, the demand for artificial lighting at night has increased. While it has brought convenience to human society, it has also led to an increase in the density and extent of artificial lighting at night in both natural and urban environments, causing an increasing problem of light pollution [72]. Light pollution not only affects global environmental change in terrestrial, coastal, and marine ecosystems [73], but also has a variety of harmful effects on plant and animal health and human health [74,75]. There is also the problem of wasted energy and money due to the increasing dependence of humans on artificial light at night [76]. In terms of animals, insects, and birds, light pollution can interfere with their behavior, sleep, reproduction, and distribution, thus affecting their habits. Artificial lighting at night has a negative impact on plant photosynthesis processes and nocturnal pollination, which leads to ecological imbalances. Humans are not immune to the effects of light pollution, which not only affects the visual perception system of the human eye, but also the sleep cycle, thereby increasing risks for many diseases. Therefore, identifying the priorities and highlights of urban lighting construction according to the activities of people and production conditions of different functional sites at night, avoiding excessive use of confusing and overly bright lights, and installing devices such as fixers and dimmers to reduce light intrusion or spillage, make it possible to implement eco-lighting in practice and radically reduce the level of light pollution.

In addition, we discuss the impact of COVID-19 on urbanization. It has been shown that COVID-19 has had a serious impact on China's socio-economic and human activities, requiring guidance for the prevention and control of the epidemic and the resumption of work and production [77,78]. In terms of the research cycle in Xiamen, the data show that the first quarter of 2020 was down 3.2%, but better than the province as a whole, with growth of 0.6% in the first half of the year, turning from negative to positive. It shows that the tourism and leisure industries "stopped" several times in the early stages of the epidemic, with factories shutting down as well as some home orders [79], causing a slowdown in growth overall. However, in 2020, Xiamen's GDP grew by 5.7% compared to the previous year, with the primary sector increasing by 2.5%, the secondary sector increasing by 6.1%, and the tertiary sector increasing by 5.5% [80], still maintaining high quality economic development. Therefore, no significant effect of COVID-19 on Xiamen has been found, and we can discuss this issue further in the future.

#### 4.2. Urban Development Proposals

The analysis in this paper shows that Xiamen has experienced rapid urban development over the past 30 years, with the city's center of gravity shifting from the island to outside of the island, achieving a shift from "city on the sea" to "sea in the city." This paper explores the distribution and evolutionary characteristics of Xiamen's urban expansion, which is important for the implementation of relevant policies and the narrowing of the gap between the inner and outer islands. In the future, Xiamen's urban development should continue to promote cross-island development from a higher station and in a broader context, accelerating the transformation from an island-based to a bay-based city.

Due to the limited space for urban development on the island of Xiamen, we should first learn from the experience of cities such as Shenzhen and improve land renewal and other related policies [81]. The following step should be to accelerate the construction and transformation of urban villages and optimize the industrial structure with a focus on tourism, science and innovation, and financial industries. The goal is to achieve high-quality, efficient development within the limited space of the island.

In terms of off-island development, the first action to take is to continue to promote the integrated development of off-island clusters of industries and cities, to promote the development of new industries led by the optoelectronics, software, and biopharmaceutical industries [82], and to accelerate the construction of a modern industrial system. The second action to take is to strengthen the industrialization and urbanization of rural areas and promote the coordinated economic and social development of urban and rural areas.

Next, the focus should be on strengthening the large-scale development and construction of new town areas and increasing the coverage of infrastructure support to accelerate the integration of the island and beyond. Finally, we should combine Xiamen's urban characteristics with ecological and environmental protection to promote the healthy and sustainable development of the city. In the context of sustainable development, healthy and environmentally friendly urban development plays an important role in enhancing the livability and attractiveness of the city. The construction of solar street lighting and carbon-neutral plazas, among others, will increase the recycling of energy; the construction of community parks, healthy trails and other green transport will be vigorously pursued according to the actual situation of each location, encouraging residents and visitors to make low-carbon trips and actively use urban public space [83]; the relevant technologies and design methods of urban lighting will be continuously improved and optimized, using LED dimming technology to dim or turn off lights [84,85], promote the conservation and recycling of resources, and reduce the impact of light pollution.

In addition, it should further strengthen regional synergistic development, vigorously promote the construction of the Xiamen–Zhangzhou–Quanzhou metropolitan area [42], deepen exchanges and cooperation with Taiwan, actively explore the synergistic development of the cross-strait economy, closely integrate with the Yangtze River Delta and GBA two major city groups in terms of industrial integration [86], resource sharing, and transport infrastructure, and actively promote investment and trade cooperation using resources such as the “One Belt, One Road” and BRICS innovation bases, so as to comprehensively enhance Xiamen's urban capacity and core competitiveness.

## 5. Conclusions

Based on the NTL data, we study and analyze the spatiotemporal variations in the urban development of Xiamen. The results lead to the following main conclusions: (1) The corrected NTL data resolve the time-scale incompatibility between DMSP/OLS and NPP/VIIRS data, improve the stability and continuity of the data, reduce the oversaturation phenomenon of NTL images of urban centers, nullify the overflow of NTL in vegetation and water areas, and increase the accuracy of data extracted from built-up areas. (2) During the period 1995–2020, the urban spatial expansion of Xiamen was mainly centered on the inner part of the island (Siming and Huli) and then expanded to the outer part of the island (Haicang, Jimei, Xiang'an, and Tong'an). During the period 2005–2020, the UB accounted for 79.44% of the total urban expansion over the entire study period, indicating that Xiamen's urban expansion was primarily concentrated between 2005 and 2020. (3) Over the whole study period, the urban center of gravity of the Xiamen's UB migrates 8757.15 m in the direction of 74.88° northeast, for a migration speed of 350.29 m/year. The urban center of gravity moved the fastest from 2005 to 2010, during which time it moved off the island. (4) The overall development level of Xiamen city increased over the study period. The development of Siming District and Huli District on the island approached saturation in the early phase of the study. However, the relative urban development rate of Haicang District and Jimei District off the island decreased gradually, and that of Tong'an and Xiang'an gradually increased.

Although the preliminary results of this study are good, the following deficiencies still remain: (1) Given the spatial resolution difference between the two different types of NTL data, errors are inevitable in the fitting results during data processing; (2) Although the threshold between water bodies and non-water bodies can be determined in many ways, it affects the result for water bodies; (3) Some areas such as farmland and green space have not been completely purged of light, and errors regarding land-use data affect the results of the study. In future research, NTL data can be combined with real-world three-dimensional data, point-of-interest data, and other multisource data to deeply mine the three-dimensional information regarding the city and explore urbanization features in greater detail. The results of the analysis may also be combined with the entity data to visualize the data.

**Author Contributions:** C.C. was primarily responsible for the conception and design of the paper, analysis of the results, and writing of the manuscript; Y.H., P.Y., Y.Z. and Z.C. made meaningful suggestions and revised the manuscript; M.F. and Y.L. were primarily responsible for data acquisition and data processing. All authors have read and agreed to the published version of the manuscript.

**Funding:** The study was supported by the Key Research and Development Program Project of Ningxia (grant no. 2021BEG03001), Natural Science Foundation of Fujian Province (grant no. 2020J01263, 2020J05232 and 2022J011229), Open Fund Project of Hunan Key Laboratory for remote sensing of the ecological environment in Dongting Lake Area (grant no. DTH Key Lab. 2021004 and 2021024).

**Institutional Review Board Statement:** Not applicable.

**Informed Consent Statement:** Not applicable.

**Data Availability Statement:** The corresponding author can provide access to the study's data upon request. It is not publicly available because it is currently being used in relevant research projects.

**Acknowledgments:** The authors sincerely thank Xiaorong Wang, the teachers and the anonymous reviewers from Xiamen University of Technology for their constructive suggestions, which vastly improved the quality of the original manuscript.

**Conflicts of Interest:** The authors declare no conflict of interest.

## References

- Bai, X.; Chen, J.; Shi, P. Landscape Urbanization and Economic Growth in China: Positive Feedbacks and Sustainability Dilemmas. *Environ. Sci. Technol.* **2012**, *46*, 132–139. [[CrossRef](#)] [[PubMed](#)]
- Bhatta, B.; Saraswati, S.; Bandyopadhyay, D. Quantifying the degree-of-freedom, degree-of-sprawl, and degree-of-goodness of urban growth from remote sensing data. *Appl. Geogr.* **2010**, *30*, 96–111. [[CrossRef](#)]
- China's National Bureau of Statistics. Available online: [http://www.stats.gov.cn/tjsj/tjgb/rkpcgb/qgrkpcgb/202106/t20210628\\_1818826.html](http://www.stats.gov.cn/tjsj/tjgb/rkpcgb/qgrkpcgb/202106/t20210628_1818826.html) (accessed on 15 October 2021).
- Deng, J.; Ke, W.; Yang, H.; Qi, J. Spatio-temporal dynamics and evolution of land use change and landscape pattern in response to rapid urbanization. *Landsc. Urban Plan.* **2009**, *92*, 187–198. [[CrossRef](#)]
- Xiao, J.; Shen, Y.; Ge, J.; Tateishi, R.; Tang, C.; Liang, Y.; Huang, Z. Evaluating urban expansion and land use change in Shi-jiazhuang, China, by using GIS and remote sensing. *Landsc. Urban Plan.* **2006**, *75*, 69–80. [[CrossRef](#)]
- Grimm, N.B.; Faeth, S.H.; Golubiewski, N.E.; Redman, C.L.; Wu, J.; Bai, X.; Briggs, J.M. Global Change and the Ecology of Cities. *Science* **2008**, *319*, 756–760. [[CrossRef](#)]
- Yang, K.; Zhang, S.; Luo, Y.; Xu, Q.; Qu, L. The widening urbanization gap between the Three Northeast Provinces and the Yangtze River Delta under China's economic reform from 1984 to 2014. *Int. J. Sustain. Dev. World Ecol.* **2018**, *25*, 262–275. [[CrossRef](#)]
- Elvidge, C.D.; Ziskin, D.; Baugh, K.E.; Tuttle, B.T.; Ghosh, T.; Pack, D.W.; Erwin, E.H.; Zhizhin, M. A Fifteen Year Record of Global Natural Gas Flaring Derived from Satellite Data. *Energies* **2009**, *2*, 595–622. [[CrossRef](#)]
- Liu, Z.; He, C.; Zhang, Q.; Huang, Q.; Yang, Y. Extracting the dynamics of urban expansion in China using DMSP-OLS nighttime light data from 1992 to 2008. *Landsc. Urban Plan.* **2012**, *106*, 62–72. [[CrossRef](#)]
- Zou, J.; Chen, Y.; Tian, J.; Wang, T. Construction of the Calibration Model for DMSP/OLS Nighttime Light Images Based on ArcGIS. *J. Geomat.* **2014**, *39*, 33–37.
- Cao, Z.; Wu, Z.; Kuang, Y.; Huang, N. Correction of DMSP/OLS Night-time Light Images and Its Application in China. *Geogr. Inf. Sci.* **2015**, *17*, 1092–1102.
- Zhang, Q.; Schaaf, C.; Seto, K.C. The Vegetation Adjusted NTL Urban Index: A new approach to reduce saturation and increase variation in nighttime luminosity. *Remote Sens. Environ.* **2013**, *129*, 32–41. [[CrossRef](#)]
- Wu, J.; Li, S.; Zhang, X. Research on saturation correction for long-time series of DMSP-OLS nighttime light dataset in China. *J. Remote Sens.* **2018**, *22*, 621–632.
- Xu, W.; Liang, J. Saturation correction method of DMSP/OLS nighttime lights image based on compound exponential model. *Geogr. Inf. Sci.* **2020**, *22*, 2227–2237.
- Li, X.; Li, D.; Xu, H.; Wu, C. Intercalibration between DMSP/OLS and VIIRS night-time light images to evaluate city light dynamics of Syria's major human settlement during Syrian Civil War. *Int. J. Remote Sens.* **2017**, *38*, 5934–5951. [[CrossRef](#)]
- Dong, H.; Li, R.; Li, J.; Li, S. Study on urban spatiotemporal expansion pattern of three first-class urban agglomerations in China derived from integrated DMSP-OLS and NPP-VIIRS nighttime light data. *Geogr. Inf. Sci.* **2020**, *22*, 1161–1174.
- Liang, L.; Bian, J.; Li, A.; Feng, W.; Lei, G.; Zhang, Z.; Zuo, J. Consistent intercalibration of nighttime light data between DMSP/OLS and NPP/VIIRS in the China-Pakistan Economic Corridor. *J. Remote Sens.* **2020**, *24*, 149–160.
- Zhang, B.; Li, J.; Wang, M.; Duan, P. Mutual Correction of DMSP/OLS and NPP/VIIRS in Mainland China. *Remote Sens. Inf.* **2021**, *36*, 99–107.

19. Zheng, Q.; Weng, Q.; Wang, K. Developing a new cross-sensor calibration model for DMSP-OLS and Suomi-NPP VIIRS night-light imageries. *ISPRS J. Photogramm. Remote Sens.* **2019**, *153*, 36–47. [[CrossRef](#)]
20. Croft, T.A. Nighttime Images of the Earth from Space. *Sci. Am.* **1978**, *239*, 86–98. [[CrossRef](#)]
21. Milesi, C.; Elvidge, C.D.; Nemani, R.R.; Running, S.W. Assessing the environmental impacts of human settlements using satellite data. *Manag. Environ. Qual.* **2003**, *14*, 99–107. [[CrossRef](#)]
22. Wang, C.; Wang, H.; Li, C.; Dong, R. Analysis of the spatial expansion characteristics of major urban agglomerations in China using DMSP/OLS images. *Acta Ecol. Sin.* **2012**, *32*, 942–954. [[CrossRef](#)]
23. Imhoff, M.L.; Lawrence, W.T.; Stutzer, D.C.; Elvidge, C.D. A technique for using composite DMSP/OLS “City Lights” satellite data to map urban area. *Remote Sens. Environ.* **1997**, *61*, 361–370. [[CrossRef](#)]
24. Shu, S.; Yu, B.; Wu, J.; Liu, H. Methods for Deriving Urban Built-up Area Using Night-light Data: Assessment and Application. *Remote Sens. Technol. Appl.* **2011**, *26*, 169–176.
25. He, C.; Shi, P.; Li, J.; Jin, C.; Pan, Y.; Jing, L.; Li, Z.; Ichinose, T. Restoring urbanization process in China in the 1990s by using non-radiance-calibrated DMSP/OLS nighttime light imagery and statistical data. *Chin. Sci. Bull.* **2006**, *51*, 1614–1620. [[CrossRef](#)]
26. Chen, X.; Zhang, F.; Du, Z.; Liu, R. An Unsupervised Urban Extent Extraction Method from NPP-VIIRS Nighttime Light Data. *Remote Sens.* **2020**, *12*, 3810. [[CrossRef](#)]
27. Cao, X.; Chen, J.; Imura, H.; Higashi, O. A SVM-based method to extract urban areas from DMSP-OLS and SPOT VGT data. *Remote Sens. Environ.* **2009**, *113*, 2205–2209. [[CrossRef](#)]
28. Zhang, Q.; Wang, P.; Chen, H.; Huang, Q.; Jiang, H.; Zhang, Z.; Zhang, Y.; Luo, X.; Sun, S. A novel method for urban area extraction from VIIRS DNB and MODIS NDVI data: A case study of Chinese cities. *Int. J. Remote Sens.* **2017**, *38*, 6094–6109. [[CrossRef](#)]
29. Xu, T.; Coco, G.; Gao, J. Extraction of urban built-up areas from nighttime lights using artificial neural network. *Geocarto Int.* **2019**, *35*, 1049–1066. [[CrossRef](#)]
30. Lu, D.; Tian, H.; Zhou, G.; Ge, H. Regional mapping of human settlements in southeastern China with multisensor remotely sensed data. *Remote Sens. Environ.* **2008**, *112*, 3668–3679. [[CrossRef](#)]
31. Liu, Z.; Zhang, Q.; Yue, D.; Hao, Y.; Su, K. Extraction of urban built-up areas based on Sentinel-2A and NPP-VIIRS nighttime light data. *Remote Sens. Land Resour.* **2019**, *31*, 227–234.
32. Sharma, R.C.; Tateishi, R.; Hara, K.; Gharechelou, S.; Iizuka, K. Global mapping of urban built-up areas of year 2014 by combining MODIS multispectral data with VIIRS nighttime light data. *Int. J. Digit. Earth* **2016**, *9*, 1004–1020. [[CrossRef](#)]
33. Yan, Q.; Li, F.; Li, L. Research on built-up area extraction via brightness correction indexes based on two kinds of nighttime light images. *Geogr. Inf. Sci.* **2020**, *22*, 1714–1724.
34. Zheng, Y.; Tang, L.; Wang, H. An improved approach for monitoring urban built-up areas by combining NPP-VIIRS nighttime light, NDVI, NDWI, and NDBI. *J. Clean. Prod.* **2021**, *328*, 129488. [[CrossRef](#)]
35. Lin, J.; Liu, X.; Li, K.; Li, X. A maximum entropy method to extract urban land by combining MODIS reflectance, MODIS NDVI, and DMSP-OLS data. *Int. J. Remote Sens.* **2014**, *35*, 6708–6727. [[CrossRef](#)]
36. Yu, B.; Tang, M.; Wu, Q.; Yang, C.; Deng, S.; Shi, K.; Peng, C.; Wu, J.; Chen, Z. Urban Built-Up Area Extraction from Log-Transformed NPP-VIIRS Nighttime Light Composite Data. *IEEE Geosci. Remote Sens. Lett.* **2018**, *15*, 1279–1283. [[CrossRef](#)]
37. Goldblatt, R.; Stuhlmacher, M.F.; Tellman, B.; Clinton, N.; Hanson, G.; Georgescu, M.; Wang, C.; Serrano-Candela, F.; Khandelwal, A.K.; Cheng, W.H.; et al. Using Landsat and nighttime lights for supervised pixel-based image classification of urban land cover. *Remote Sens. Environ.* **2018**, *205*, 253–275. [[CrossRef](#)]
38. Omurakunova, G.; Bao, A.; Jiapaer, G.; Khan, G.; Jiang, L.; Jolochieva, E. Urban growth dynamics during the period 1992–2013 in Kyrgyzstan based on DMSP-OLS nightlight satellite data. *Arab. J. Geosci.* **2021**, *14*, 1959. [[CrossRef](#)]
39. Liu, F.; Zhang, Z.; Shi, L.; Zhao, X.; Xu, J.; Yi, L.; Liu, B.; Wen, Q.; Hu, S.; Wang, X.; et al. Urban expansion in China and its spatial-temporal differences over the past four decades. *J. Geogr. Sci.* **2016**, *26*, 1477–1496. [[CrossRef](#)]
40. Frohling, S.; Milliman, T.; Seto, K.C.; Friedl, M.A. A global fingerprint of macro-scale changes in urban structure from 1999 to 2009. *Environ. Res. Lett.* **2013**, *8*, 024004. [[CrossRef](#)]
41. Zheng, Y.; He, Y.; Zhou, Q.; Wang, H. Quantitative Evaluation of Urban Expansion using NPP-VIIRS Nighttime Light and Landsat Spectral Data. *Sustain. Cities Soc.* **2022**, *76*, 103338. [[CrossRef](#)]
42. Jiang, Y.; Sun, S.; Zheng, S. Exploring Urban Expansion and Socioeconomic Vitality Using NPP-VIIRS Data in Xia-Zhang-Quan, China. *Sustainability* **2019**, *11*, 1739. [[CrossRef](#)]
43. Zhao, S.; Zhou, D.; Zhu, C.; Qu, W.; Zhao, J.; Sun, Y.; Huang, D.; Wu, W.; Liu, S. Rates and patterns of urban expansion in China’s 32 major cities over the past three decades. *Landsc. Ecol.* **2015**, *30*, 1541–1559. [[CrossRef](#)]
44. Schneider, A.; Woodcock, C.E. Compact, Dispersed, Fragmented, Extensive? A Comparison of Urban Growth in Twenty-five Global Cities using Remotely Sensed Data, Pattern Metrics and Census Information. *Urban Stud.* **2008**, *45*, 659–692. [[CrossRef](#)]
45. Zhou, L.; Shi, P.; Chen, J.; Toshiaki, I. Application of Compound Night Light Index Derived from DMSP/OLS Data to Urbanization Analysis in China in the 1990s. *Acta Geogr. Sin.* **2003**, *58*, 893–902.
46. Li, L.; Gong, J.; Yang, J.; Li, S. Urban Spatial Pattern Evolution of Wuhan City Based on Nighttime Light. *Remote Sens. Inf.* **2017**, *32*, 133–141.
47. Alahmadi, M.; Atkinson, P.M. Three-Fold Urban Expansion in Saudi Arabia from 1992 to 2013 Observed Using Calibrated DMSP-OLS Night-Time Lights Imagery. *Remote Sens.* **2019**, *11*, 2266. [[CrossRef](#)]

48. Rafael, C.; Martin, D.A.; Vargas, J.F. Measuring the size and growth of cities using nighttime light. *J. Urban Econ.* **2021**, *125*, 103254.
49. Xiamen Bureau of Statistics. Available online: [http://tjj.xm.gov.cn/tjzl/ndgb/202105/t20210527\\_2554550.htm](http://tjj.xm.gov.cn/tjzl/ndgb/202105/t20210527_2554550.htm) (accessed on 10 January 2022).
50. Xiamen Bureau of Statistics. Available online: [http://tjj.xm.gov.cn/tjzl/tjsj/jdsj/sjyb/202201/t20220127\\_2623790.htm](http://tjj.xm.gov.cn/tjzl/tjsj/jdsj/sjyb/202201/t20220127_2623790.htm) (accessed on 12 March 2022).
51. Li, Y.; Geng, X. *RS Based Quantitative Analysis of Urban Environment: Application of Remote Sensing in Xiamen City*; Peking University Press: Beijing, China, 2019.
52. Xiamen Bureau of Statistics. Available online: [http://tjj.xm.gov.cn/tjzl/ndgb/201803/t20180328\\_2091029.htm](http://tjj.xm.gov.cn/tjzl/ndgb/201803/t20180328_2091029.htm) (accessed on 15 June 2022).
53. Haixi Sunnews. Available online: [http://dzb.sunnews.cn/html/2020-10/14/content\\_788624.htm?div=-1](http://dzb.sunnews.cn/html/2020-10/14/content_788624.htm?div=-1) (accessed on 10 July 2021).
54. Xiamen Daily. Available online: <https://epaper.xmnn.cn/xmrb/20200518/> (accessed on 18 July 2021).
55. Zheng, Y.; Shao, G.; Tang, L.; He, Y.; Wang, X.; Wang, Y.; Wang, H. Rapid Assessment of a Typhoon Disaster Based on NPP-VIIRS DNB Daily Data: The Case of an Urban Agglomeration along Western Taiwan Straits, China. *Remote Sens.* **2019**, *11*, 1709. [[CrossRef](#)]
56. Elvidge, C.D.; Baugh, K.E.; Kihn, E.A.; Kroehl, H.W.; Davis, E.R.; Davis, C.W. Relation between satellite observed visible near infrared emissions, population, economic activity and electric power consumption. *Int. J. Remote Sens.* **1997**, *18*, 1373–1379. [[CrossRef](#)]
57. Forbes, D.J. Multi-scale analysis of the relationship between economic statistics and DMSP-OLS night light images. *GIScience Remote Sens.* **2013**, *50*, 483–499. [[CrossRef](#)]
58. Zheng, Y.; Zhou, Q.; He, Y.; Wang, C.; Wang, X.; Wang, H. An Optimized Approach for Extracting Urban Land Based on Log-Transformed DMSP-OLS Nighttime Light, NDVI, and NDWI. *Remote Sens.* **2021**, *13*, 766. [[CrossRef](#)]
59. Imhoff, M.L.; Lawrence, W.T.; Elvidge, C.; Paul, T.; Levine, E.; Privalsky, M.V.; Brown, V. Using nighttime DMSP/OLS images of city lights to estimate the impact of urban land use on soil resources in the United States. *Remote Sens. Environ.* **1997**, *59*, 105–117. [[CrossRef](#)]
60. Shao, G.; Tang, L.; Zhang, H. Introducing Image Classification Efficacies. *IEEE Access* **2021**, *9*, 134809–134816. [[CrossRef](#)]
61. Shao, G.; Tang, L.; Liao, J. Overselling overall map accuracy misinforms about research reliability. *Landsc. Ecol.* **2019**, *34*, 2487–2492. [[CrossRef](#)]
62. Wu, W.; Zhao, S.; Zhu, C.; Jiang, J. A comparative study of urban expansion in Beijing, Tianjin and Shijiazhuang over the past three decades. *Landsc. Urban Plan.* **2015**, *134*, 93–106. [[CrossRef](#)]
63. Yang, C.; Li, Q.; Hu, Z.; Chen, J.; Shi, T.; Ding, K.; Wu, G. Spatiotemporal evolution of urban agglomerations in four major bay areas of US, China and Japan from 1987 to 2017: Evidence from remote sensing images. *Sci. Total Environ.* **2019**, *671*, 232–247. [[CrossRef](#)]
64. Wu, J.; He, S.; Peng, J.; Huang, X.; Zhang, L. Research on Spatial Characteristics of Urban Development Based on DMSP-OLS Data. *Geogr. Inf. Sci.* **2014**, *30*, 20–25.
65. Liu, L. Urban sprawl metrics based on nighttime light data for metropolitan areas. *Remote Sens. Land Resour.* **2018**, *30*, 208–213.
66. Yang, Y.; Ma, M.; Ge, W. Spatial characteristics of urban development in Beijing using nighttime light data. *Remote Sens. Inf.* **2019**, *34*, 41–50.
67. Zhan, X.; Pan, W.; Cai, Y.; Zheng, P. Research of urban expansion measures based on multi-source remote sensing data—A case study of Xiamen City. *J. Fuzhou Univ. Nat. Sci. Ed.* **2017**, *45*, 355–361.
68. Liu, Y.; Yin, G.; Ma, L.J. Local state and administrative urbanization in post-reform China: A case study of Hebi City, Henan Province. *Cities* **2012**, *29*, 107–117. [[CrossRef](#)]
69. Yearbook of Xiamen Special Economic Zone. Available online: <https://www.xm.gov.cn/zw/gk/tqjj/xmjqtqj/> (accessed on 20 June 2022).
70. Silva, P.; Li, L. Mapping Urban Expansion and Exploring Its Driving Forces in the City of Praia, Cape Verde, from 1969 to 2015. *Sustainability* **2017**, *9*, 1434. [[CrossRef](#)]
71. Gong, J.; Hu, Z.; Chen, W.; Liu, Y.; Wang, J. Urban expansion dynamics and modes in metropolitan Guangzhou, China. *Land Use Policy* **2018**, *72*, 100–109. [[CrossRef](#)]
72. Rajkhowa, R. Light pollution and impact of light pollution. *Int. J. Sci. Res.* **2014**, *3*, 861–867.
73. Lyytimäki, J. Nature’s nocturnal services: Light pollution as a non-recognised challenge for ecosystem services research and management. *Ecosyst. Serv.* **2013**, *3*, e44–e48. [[CrossRef](#)]
74. Chepesiuk, R. Missing the Dark: Health Effects of Light Pollution. *Environ. Health Perspect.* **2009**, *117*, A20–A27. [[CrossRef](#)]
75. Zielinska-Dabkowska, K.M.; Szlachetko, K.; Bobkowska, K. An Impact Analysis of Artificial Light at Night (ALAN) on Bats. A Case Study of the Historic Monument and Natura 2000 Wisloui’scie Fortress in Gdansk, Poland. *Int. J. Environ. Res. Public Health* **2021**, *18*, 11327. [[CrossRef](#)]
76. Komal, K.; Soumya, N.; Arif, A. Studying light pollution as an emerging environmental concern in India. *J. Urban Manag.* **2022**, *11*, 392–405.
77. Yang, W.; Wang, X.; Zhang, K.; Ke, Z. COVID-19, Urbanization Pattern and Economic Recovery: An Analysis of Hubei, China. *Int. J. Environ. Res. Public Health* **2020**, *17*, 9577. [[CrossRef](#)]

78. Shao, Z.; Tang, Y.; Huang, X.; Li, D. Monitoring work resumption of wuhan in the COVID-19 epidemic using 261 daily nighttime light. *Photogramm. Eng. Remote Sens.* **2021**, *87*, 197–206. [CrossRef]
79. Tian, H.; Liu, Y.; Li, Y.; Wu, C.-H.; Chen, B.; Kraemer, M.U.G.; Li, B.; Cai, J.; Xu, B.; Yang, Q.; et al. An investigation of transmission control measures during the first 50 days of the COVID-19 epidemic in China. *Science* **2020**, *368*, 638–642. [CrossRef] [PubMed]
80. Yearbook of Xiamen Special Economic Zone. Available online: <https://www.xm.gov.cn/zfxgk/xgkznm/gmzgan/tjnj/> (accessed on 25 July 2022).
81. People.cn. Available online: <http://fj.people.com.cn/n2/2022/0620/c181466-40002275.html> (accessed on 25 June 2022).
82. Fujian Development and Reform Commission. Available online: [https://fgw.fujian.gov.cn/zwgk/xwdt/sxd/202207/t20220705\\_5946182.htm](https://fgw.fujian.gov.cn/zwgk/xwdt/sxd/202207/t20220705_5946182.htm) (accessed on 4 July 2022).
83. Zielinska-Dabkowska, K.M.; Bobkowska, K. Rethinking Sustainable Cities at Night: Paradigm Shifts in Urban Design and City Lighting. *Sustainability* **2022**, *14*, 6062. [CrossRef]
84. De Miguel, A.S.; Bennie, J.; Rosenfeld, E.; Dzurjak, S.; Gaston, K.J. First Estimation of Global Trends in Nocturnal Power Emissions Reveals Acceleration of Light Pollution. *Remote Sens.* **2021**, *13*, 3311. [CrossRef]
85. LED Lighting and Dark Skies. Available online: <http://www.flagstaffdarkskies.org/led-lighting-dark-skies/> (accessed on 25 July 2022).
86. Xiamen Municipal People’s Government. Available online: [http://www.xm.gov.cn/zt/xgddsjjlzhjs/pljd/202206/t20220614\\_2667272.htm](http://www.xm.gov.cn/zt/xgddsjjlzhjs/pljd/202206/t20220614_2667272.htm) (accessed on 25 June 2022).